Supercond. Sci. Technol. 4 (1991) 583–586. Printed in the UK

Characterization of $YBa_2Cu_3O_7$ step-edge Josephson junctions

K Herrmann, Y Zhang, H-M Mück, J Schubert, W Zander and A I Braginski

Institut für Schicht und Ionentechnik (ISI), Forschungszentrum Jülich (KFA), Postfach 1913, D-W5170 Jülich, Federal Republic of Germany

Abstract. We have fabricated and characterized thin film $YBa_2Cu_3O_7$ step-edge microbridges for application in SQUIDS. Epitaxial YBCO films were pulsed-laser-deposited on $SrTiO_3$ and had T_c's of 88–90 K. Sharp steps in $SrTiO_3$ were obtained by photolithographic techniques and Ar ion milling with step heights (h) between 100 and 250 mm. We investigated step-edge junctions (SEJ) with different film thicknesses (d) from 100 to 250 mm but with a constant ratio $d/h = 1$. The width of the microbridges was 2–2.5 μm. The T_c's of the bridges were 65–85 K, depending on film thickness and the duty cycle during ion milling. The I-V curves were RSJ-like and clear Shapiro steps were observed. The junction normal resistance was independent of temperature. With applied magnetic field the critical current I_c showed a T-dependent modulation, indicating that there was self-shielding and I_c non-uniformity in the junctions. Low-frequency noise measured in RF SQUIDS was relatively low. We showed that it was generated predominantly in the junctions.

1. Introduction

The step-edge weak link in a c-axis oriented $YBa_2Cu_3O_7$ (YBCO) epitaxial film represents one of several approaches to engineered active Josephson devices capable of operating at 77 K. To date, step-edge weak links, first reported by Simon *et al* [1], have mainly been characterized indirectly in RF- and DC-superconducting quantum interference devices (SQUIDS) [2–5]. The mechanism of the weak-link operation has not been determined unambiguously. The hitherto reported static current–voltage (I–V) characteristics at 4.2 K, where noise rounding can be neglected, were reminiscent of a flux-flow device rather than of a resistively-shunted junction (RSJ) behaviour [1, 4]. The observed Shapiro steps could be fitted to the RSJ model but with a normal junction resistivity, R_n, five times lower than the measured value [1].

High resolution transmission electron microscopy of YBCO films pulsed-laser deposited over 200 nm high steps in $SrTiO_3$ (step angle $\theta = 55°$–$70°$) has revealed the following microstructural features: (1) epitaxial, i.e. orthogonal to film plane, growth habit of c-axis YBCO over the step, (2) the resulting nucleation of two clean 90° grain boundaries (GBS) at the step edges, of approximately (103) orientation, and (3) an occasional, relatively rare occurrence of other defects such as dirty grain boundaries and lamellar second phase (e.g. 211) intergrowths [6]. The film thickness on the step was 50–70% of that of the planar film. However, on steeper steps, especially when $\theta > 80°$, a local constriction was present in the film near the lower corner of the step and the orientation of the lower grain boundary tended to approach the (100) plane [7]. Generally, the current path over the step is thus always along the $Cu–O_2$ planes and intersects two 90° grain boundaries. At not too steep angles, i.e. in absence of a constriction in the film over the step, the path is unlikely to be of filamentary nature. However, when a constriction is present, this may, indeed, be the case. Depending upon the step angle, therefore, two different modes of the weak-link operation might be prevalent.

2. Sample fabrication

Here, we report on characteristics of weak links fabricated on 60°–65° steps and having the nearly optimal [8] film thickness to step-height ratio, d/h, equal to one. The fabrication method has been described earlier in some detail [8]. Briefly, steps in $SrTiO_3$ and $LaAlO_3$ were Ar^+ ion-etched through photolithographic metal (Nb) masks. Step heights ranged typically between 100 and 250 nm. The step angle was controlled by the angle of incidence of ion beam onto the rotating sample holder. After stripping the mask, the substrate was annealed for 1 h at 1000 °C in flowing O_2 to remove the surface damage caused by ion bombardment. The YBCO film was grown by pulsed laser deposition using a standard procedure [9] and patterned by optical lithography. Pattern transfer occurred by Ar^+ ion-beam etching (IBE) at a beam energy of 500 eV, ion current density of 0.5 mA cm^{-2}, 30–50% duty cycle and cooling of the rotating chip holder to -5 °C in order to prevent an excessive heating of the chip and resulting loss of oxygen from YBCO. The 10 × 10 mm chips were pasted onto the holder with vacuum grease.

0953-2048/91/110583 + 04 $03.50

Two test chip designs have been used. Four single bridges over steps, a reference bridge without any step and four RF SQUID washers were present on the first test chip. Each 1.4 × 1.4 mm washer contained a double weak link in series since its microbridge was positioned over a local 5 μm wide groove in the substrate. All microbridges were nominally $w = 2$ μm wide and 10 μm long. In a fabricated chip, the bridge width was typically 2.0–2.5 μm. Each washer's hole was 100 × 100 μm corresponding to an inductance of approximately 125 pH. The chip had 16 pads for four-point transport measurements. Contacting was done either with spring-loaded contacts or by wire bonding. The second, earlier chip design consisted of 16 RF SQUID washers, practically identical to those of the first design, which were positioned over single steps extending across the whole substrate [3, 8]. Consequently, a 0.65 mm wide step extended across each washer's body and the RF-current path. The microbridges were 1 and 2 μm wide.

3. Results

The four-point DC and low-frequency (< 100 Hz) transport measurements were performed mostly in He-flow cryostats. The RF SQUIDS were evaluated in Mumetal shielded probes as described in [3, 8]. The temperature measurements were carried out using Pt and Ge thermometers. The reference bridges (without a step) had a T_c ($R = 0$) of 89–90 K. At 77 K and 10 nV across the bridge, the self-field critical current density, J_c, was 2–6 × 10^6 A cm^{-1} on $SrTiO_3$ and up to 2 × 10^7 A cm^{-2} on $LaAlO_3$. These results refer to YBCO film thicknesses between $d = 100$ and 250 nm. The $R(T)$ measurements of microbridges across steps indicated that their T_c was reduced to 65–85 K. One cause of this reduction was a material degradation, since T_c decreased with the increasing ion-etching duty cycle. The degradation was tentatively attributed to still insufficient cooling during etching and the resulting oxygen loss from the bridge surface on the step where Cu–O_2 planes terminate [6]. However, at 77 K, the washer structures exhibited a clear SQUID response even if a small finite resistance tail was observed above 65 K in single weak links on the same chip. Consequently, an additional possible cause of T_c reduction was the phase slip in the junction.

The examples of weak-link I–V characteristics measured at 4.2 K are shown in figure 1 for two levels of critical current: (a) $I_c = 0.2$ mA and (b) 2 mA. Links with critical currents another order of magnitude higher could not be measured at 4.2 K since the required currents exceeded the contact capability. Overall, the weak-link J_c could be varied by up to three orders of magnitude, depending upon the step angle and height, and the film thickness to step-height ratio. Electron microscopy shows that these geometrical variables determine the microstructure. The orientation of the lower grain boundary, and the presence of a constriction mentioned above [7] particularly depend upon these variables. In turn, such microstructural changes can be expected to affect the J_c.

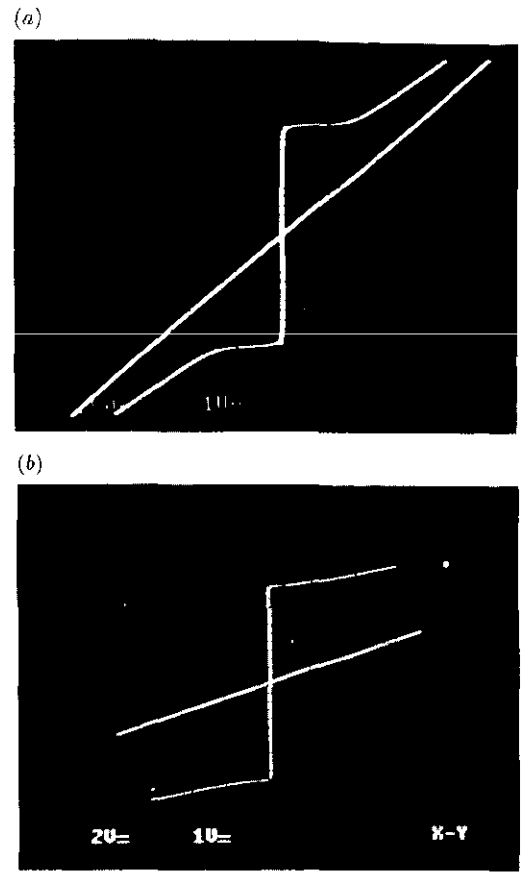

Figure 1. Current–voltage characteristics, at 4.2 K, of two weak links with different levels of I_c: (*a*) 0.2 mA and (*b*) 2.1 mA.

The low-temperature I–V characteristics shown are virtually free of thermal noise-rounding and can be described by the resistive shunted junction model (RSJ) with some excess current. Generally, the deviation from RSJ behaviour was found to increase with the I_c level, i.e. the strength of coupling. When I_c was another order of magnitude above that of figure 1(*b*), the I–V characteristics ($T > 4.2$ K) were of the flux-flow type. The slopes of straight lines in figure 1 define the junctions' normal

Table 1. Description of weak links of figure 1. (Data at 4.2 K, unless otherwise indicated.)

Parameter	Junction (a)	Junction (b)
Film thickness, $d = h$ (nm)	140	250
Bridge width, w (nm)	2.5	2.5
Critical T ($I_c = 0$) (K)	65	77
Critical current, I_c (mA)	0.2	2.1
Critical current density, J_c (A cm^{-2})	6.3 × 10^4	4.2 × 10^5
Reduction of film J_c, $J_{c\,\mathrm{ref}}/J_c$ at 65 K	—	70
Resistance (at 2 GHz), R_n (Ω)	3	0.56
Critical voltage $V_c = I_c R_n$ (mV)	0.6	1.2
Josephson penetration depth, λ_J (μm)	1.2	0.5
w/λ_J	2	5

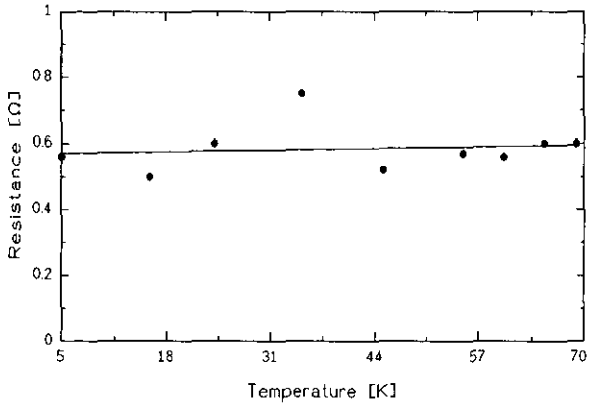

Figure 2. Weak-link (*b*) resistance against temperature (I_c suppressed by 2 GHz irradiation).

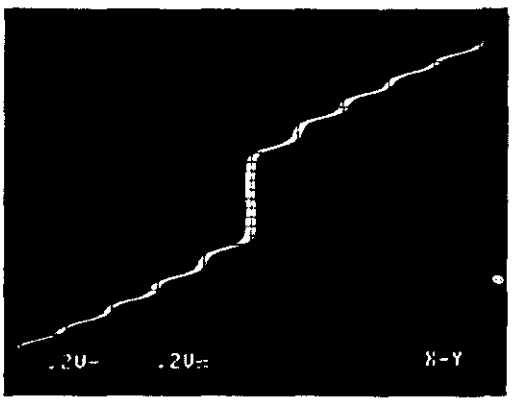

Figure 4. Current–voltage characteristic of weak link (*b*) under $f = 10.1$ GHz irradiation at 45 K.

resistance, R_n, under total supression of I_c by microwave irradiation at 2 GHz. The corresponding I_cR_n products at 4.2 K and other device data are shown in table 1. In various RSJ-like samples, I_cR_n values between 0.5 and 1.6 mV have been observed. The R_n values were temperature independent within the accuracy of the measurement, as shown in figure 2. The I_cR_n scaled with $J_c : I_cR_n\ (J_c)^p$, with $p = 0.5$ to 0.6, as in grain boundary junctions on bicrystal substrates [10] and in natural grain boundaries [11].† The resistivity of the 'barrier' was $\rho_n = 10^{-9}$ to $10^{-8}\ \Omega\ cm^2$, comparable to that of grain boundary junctions. The temperature dependence of I_c is given in figure 3 for junction (b). Near T_c, it is linear. Various weak links measured thus far exhibited a power-law dependence: $I_c = (1 - T/T_c)^n$ with values of n between 1.0 and 2.2. For junctions (a) and (b) of table 1 the J_cs at 65 K were 0 and 8.8×10^4 A cm^{-2} respectively.

Under microwave irradiation, the weak-link *I–V* characteristics exhibited well developed Shapiro steps at $V_n = nhf/2e$ where h is Planck's constant and e the electron charge, with $n = 1, 2, 3, \ldots$. Figure 4 shows the data at $T = 45$ K for sample (b). No steps at subharmonic frequencies have been recorded in this and other RSJ-type samples. Also, at higher temperatures, the critical current was modulated by the microwave current, I_{RF}. All this indicated that our step-edge devices are true Josephson junctions, i.e. their effective barrier thickness (or device length), L, is comparable to the coherence length along the $Cu–O_2$ planes, ξ_{ab}.

The modulation of critical current by magnetic field perpendicular to the film plane, H, was weak and increased with temperature, as could be expected for junctions which, at low temperatures, are wider than the Josephson penetration depth, λ_J (table 1) and thus exhibit self-shielding effects. For junction (b), the modulation was less than 10% at 4.2 K and increased to about 50% at 70 K. The observed $I_c(H)$ dependences were quite irregular, with a superposed fine structure, as shown in figure 5 for junction (b). The dependences exhibited a hysteretic behaviour indicating some flux trapping. Hence, figure 5 shows only one branch of $I_c(H)$ taken with ascending H. Here, the modulation period is roughly 16 Gauss while the calculated period is 19 Gauss, assuming that the barrier is inclined at an angle of 45° to the film plane. This can be taken as a fair agreement. However, the dissimilarity with the ideal Frauenhofer diffraction pattern indicates that the critical current density distribution in this (and other junctions') cross section is quite non-uniform. The fine structure seen in figure 5 is of unknown origin, and similar to that observed in grain-boundary junctions

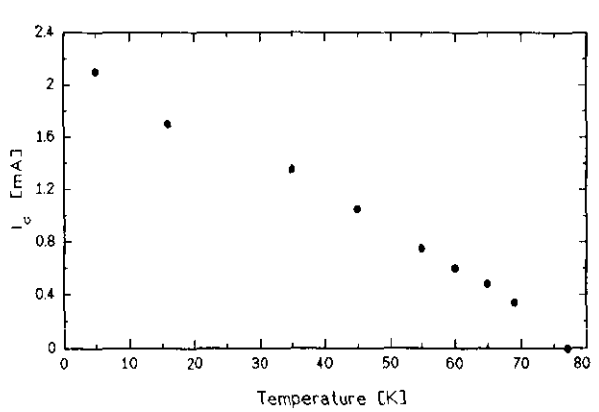

Figure 3. Temperature dependence of I_c in weak link (*b*).

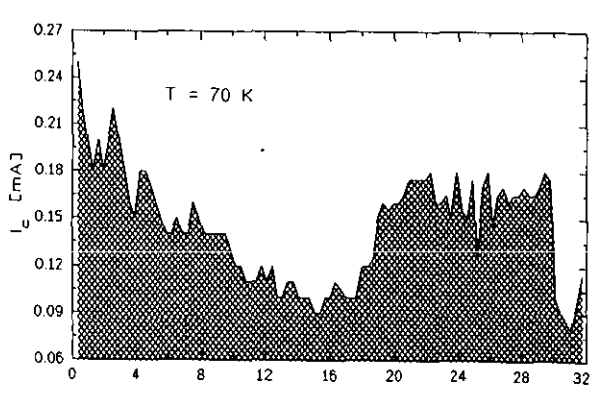

Figure 5. Critical current dependence upon applied magnetic field intensity at 70 K. Only the positive, increasing field branch is shown.

† Note added: subsequent measurement of a larger number of junctions made the scaling result rather uncertain. This point requires further clarification.

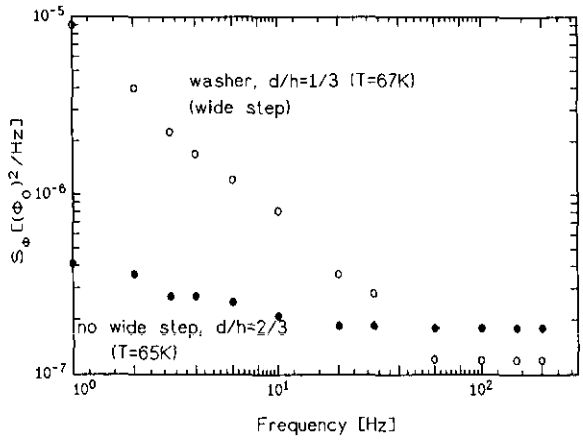

Figure 6. Low-frequency flux noise data at 66 ± 1 K for two types of washer, with and without a wide step.

[12]. One can speculate that it is related to local vortex jumps and thus to $1/f$ noise.

The low-frequency noise of step-edge junctions was evaluated in RF SQUIDs. An example of the earlier reported flux noise data against frequency, $S_\Phi(f)$ at 65 K [3, 8], determined in structures with a wide step across the washer (the second chip design described above), is compared in figure 6 with flux noise measured in a washer without a wide step (first design). The elimination of the wide step resulted in a decrease in S_Φ at 1 Hz by more than one order of magnitude. One can thus believe that the SQUID $(1/f)$-like noise originates predominantly in the step structure, i.e. in the junction itself. The noise at 1 Hz ($6 \times 10^{-4}\Phi_0/\mathrm{Hz}^{1/2}$ at 77 K) is comparable to that measured in a DC SQUID with grain-boundary junctions on bicrystal substrates [10].

4. Concluding discussion

All the presented data point to a step-edge junction behaviour qualitatively and quantitatively similar to that of grain-boundary junctions on bicrystal substrates [10, 12] and of natural grain boundaries [11]. Observed were similar RSJ-like I–V characteristics and $I_c R_n$ products, similar junction resistivities, the temperature independence of R_n, an absence of Shapiro steps at subharmonic frequencies, field modulation with a fine structure in $I_c(H)$ characteristics, albeit with a greater J_c non-uniformity, and similar levels of $1/f$ noise.

All measured characteristics strongly suggest that step-edge devices are GB junctions. With two similar grain boundaries in series the devices could be double junctions. Alternatively, one of these GBs might be sufficiently weaker coupled than the other. The junction properties would then be defined by the weaker GB alone. At all grain boundaries on step-edges, the $Cu–O_2$ planes meet at a 90° angle but the boundary orientation varies [7]. This orientation affects the connectivity of $Cu–O_2$ planes and should, therefore, have a strong effect on J_c.

Clearly, no direct experimental proof of this is yet to hand. We are not aware of any direct investigation of such 90° grain boundaries but note that analogous grain-boundaries are present in (100) mosaic a-axis films where the c-axis directions in neighbouring domains are orthogonal. The reduction of J_c, compared with c-axis films, is by one to two orders of magnitude, similar to most of our junctions. However, Ravi *et al* [13] have calculated the free energies of various grain boundaries and suggested that certain low-energy grain boundaries should not reduce J_c significantly. It is not clear whether their considerations apply to boundaries at step edges or not. To determine experimentally the effect of various step-edge grain boundaries on J_c it would be useful to model these in films on bicrystal substrates.

Acknowledgments

We thank Professor C Heiden for useful discussions and acknowledge the support of BMFT Consortium 'First Application of HTS in Micro- and Cryoelectronics'.

References

[1] Simon RW *et al* 1991 *IEEE Trans. Magn.* **27** 3209
[2] Daly K P, Dozier W D, Burch J F, Coons S B, Hu R, Platt C E and Simon R W 1991 *Appl. Phys. Lett.* **58** 543
[3] Cui G, Zhang Y, Herrmann K, Buchal Ch, Schubert J, Zander W, Braginski A I and Heiden C 1991 *Supercond. Sci. Technol.* **4** S130
[4] Siegel M, Schmidl F, Zach K, Heinz E, Borck J, Michalke W and Seidel P 1991 *Physica* C in press
[5] Yoshii M, Kita J, Nakatsu O and Yamada Y 1991 *Japan. J. Appl. Phys.* **30** L587
[6] Jia C L, Kabius B, Urban K, Herrmann K, Cui G J, Schubert J, Zander W, Braginski A I and Heiden C 1975 *Physica* C **175** 545 and unpublished data
[7] Jia C L *et al* 1991 *Physica C* to be submitted
[8] Cui G J, Herrmann K, Zhang Y, Jia C L, Buchal Ch, Schubert J, Zander W, Braginski A I and Heiden C 1991 *Nonlinear Superconductive Electronics and Josephson Devices* (New York: Plenum) in press
[9] Stritzker B, Schubert J, Poppe U, Zander W, Kröger U, Lubig A and Buchal Ch 1990 *J. Less-Common Met.* **164 & 165** 279
[10] Gross R and Mayer B 1991 *Physica* C in press
[11] Lathrop D K, Russek S E, Moeckly B H, Chamberlain D, Pesenson L, Buhrman R A, Shin D H and Silcox J 1991 *IEEE Trans. Magn.* **27** 3203
[12] Gross R, Chaudhari P, Kawasaki M and Gupta A 1991 *IEEE Trans Magn.* **27** 3227
[13] Ravi T S, Hwang D M, Ramesh R, Chan, S-W, Nazar L, Chen C Y, Inam A and Venkatesan T 1990 *Phys. Rev.* B **42** 10141